



# Effects of pump pulse extinction ratio in Brillouin optical time-domain analysis sensors

HARITZ IRIBAS,<sup>1</sup> JON MARIÑELARENA,<sup>1</sup> CHENG FENG,<sup>2</sup> JAVIER URRICELQUI,<sup>1</sup> THOMAS SCHNEIDER,<sup>2</sup> AND ALAYN LOAYSSA<sup>1,\*</sup>

<sup>1</sup>Institute of Smart Cities, Universidad Pública de Navarra, Campus Arrosadia s/n, 31006 Iruñea, Spain

<sup>2</sup>Institut für Hochfrequenztechnik, Technische Universität Braunschweig, 38106 Braunschweig, Germany

\*alayn.loayssa@unavarra.es

**Abstract:** We report on two previously unknown non-local effects that have been found to impair Brillouin optical time-domain analysis (BOTDA) sensors that deploy limited extinction ratio (ER) pump pulses. The first one originates in the increased depletion of the pedestal of the pump pulses by the amplified probe wave, which in turn entails a reduced amplification of the probe and a measurement distortion. The second effect is due to the interplay between the transient response of the erbium-doped fiber amplifiers (EDFA) that are normally deployed to amplify the pump and the pedestal of the pump pulses. The EDFA amplification modifies the pedestal that follows the pulses in such a way that it also leads to a distortion of the measured gain spectra after normalization. Both effects are shown to lead to non-local effects in the measurements that have similar characteristics to those induced by pump pulse depletion. In fact, the total depletion factor for calculations of the Brillouin frequency shift (BFS) error in BOTDA sensors is shown to be the addition of the depletion factors linked to the pump pulse as well as the pedestal. A theoretical model is developed to analyze both effects by numerical simulation. Furthermore, the effects are investigated experimentally in long-range BOTDA sensors. The pedestal depletion effect is shown to severely constrain the probe power as well as the minimum ER of the pulses that can be deployed in BOTDA sensors. For instance, it is shown that, in a long-range dual-probe BOTDA, an ER higher than 32-dB, which is above that provided by standard electro-optic modulators (EOM), is necessary to be able to deploy a probe power of -3 dBm, which is the theoretical limit for that type of sensors. Even more severe can be the limitation due to the depletion effect induced by the EDFA transient response. It is found that the impairments brought by this effect are independent of the probe power, hence setting an ultimate limit for the BOTDA sensor performance. Experimentally, a long-range BOTDA deploying a 26-dB ER EOM and a conventional EDFA is shown to exhibit a BFS error higher than 1 MHz even for very small probe power.

© 2017 Optical Society of America

**OCIS codes:** (060.2370) Fiber optics sensors; (290.5900) Scattering, stimulated Brillouin.

## References and links

1. M. A. Soto, and L. Thévenaz, "Modeling and evaluating the performance of Brillouin distributed optical fiber sensors," *Opt. Express* **21**(25), 31347–31366 (2013).
2. M. Alem, M. A. Soto, and L. Thévenaz, "Analytical model and experimental verification of the critical power for modulation instability in optical fibers," *Opt. Express* **23**(23), 29514–29532 (2015).
3. S. Foaleng, F. Rodríguez-Barrios, S. Martín-Lopez, M. González-Herráez, and L. Thévenaz, "Detrimental effect of self-phase modulation on the performance of Brillouin distributed fiber sensors," *Opt. Lett.* **36**, 97–99 (2011).
4. L. Thévenaz, S. F. Mafang, and J. Lin, "Effect of pulse depletion in a Brillouin optical time-domain analysis system," *Opt. Express* **21**(12), 14017–14035 (2013).
5. V. Lecoeuche, D. J. Webb, C. N. Pannell, and D. A. Jackson, "Transient response in high-resolution Brillouin-based distributed sensing using probe pulses shorter than the acoustic relaxation time," *Opt. Lett.* **25**(3), 156–158 (2000).
6. A. Zornoza, D. Olier, M. Sagues, and A. Loayssa, "Brillouin distributed sensor using RF shaping of pump pulses," *Meas. Sci. Technol.* **21**(9), 094021 (2010).
7. A. Minardo, and L. Zeni, "Influence of laser phase noise on Brillouin optical time-domain analysis sensors," *Proc. SPIE* **9916**, 99162T (2016).
8. W. Li, X. Bao, Y. Li, and L. Chen, "Differential pulse-width pair BOTDA for high spatial resolution sensing," *Opt. Express* **16**(26), 21616–21625 (2008).
9. G. P. Agrawal, *Nonlinear Fiber Optics*, 5th ed. (Academic, 2013).

10. X. Bao, J. Dhliwayo, N. Heron, D. J. Webb, and D. A. Jackson, "Experimental and theoretical studies on a distributed temperature sensor based on Brillouin scattering," *J. Lightwave Technol.* **13**(7), 1340–1348 (1995).
11. A. Minardo, R. Bernini, and L. Zeni, "A simple technique for reducing pump depletion in long range distributed Brillouin fiber sensors," *IEEE Sens. J.* **9**(6), 633–634 (2009).
12. M. O. van Deventer, and A. J. Boot, "Polarization properties of stimulated Brillouin scattering in single-mode fibers," *J. Lightwave Technol.* **12**(4), 585–590 (1994).
13. A. Domínguez-López, X. Angulo-Vinuesa, A. López-Gil, S. Martín-López, and M. González-Herráez, "Non-local effects in dual-probe-sideband Brillouin optical time domain analysis," *Opt. Express* **23**(8), 10341–10352 (2015).
14. A. Domínguez-López, Z. Yang, M. A. Soto, X. Angulo-Vinuesa, S. Martín-López, L. Thévenaz and M. González-Herráez, "Novel scanning method for distortion-free BOTDA measurements," *Opt. Express* **24**(10), 10188–10204 (2016).
15. T. Shimizu, K. Nakajima, K. Shiraki, K. Ieda, and I. Sankawa, "Evaluation methods and requirements for the stimulated Brillouin scattering threshold in a single-mode fiber," *Opt. Fiber Technol.* **14**(1), 10–15 (2008).
16. Y. Sun, J. L. Zyskind, and A. K. Srivastava, "Average inversion level, modeling, and physics of erbium-doped fiber amplifiers," *IEEE J. Sel. Top. Quant.* **3**(4), 991–1007 (1997).
17. K. Y. Ko, M. S. Demokan, and H. Y. Tam, "Transient analysis of erbium-doped fiber amplifiers," *IEEE Photonics Tech. L.* **6**(12), 1436–1438 (1994).

## 1. Introduction

During the last few decades, distributed fiber optic sensors based on the Brillouin scattering nonlinear effect have been thoroughly researched mainly due to their ability to provide high precision distributed temperature and strain measurements over extremely large structures. The most successful Brillouin distributed sensors to date are based on the Brillouin optical time-domain analysis (BOTDA) technique, where a pump pulse and a counter-propagating continuous-wave (CW) probe interact in the sensing fiber under test (FUT). Initial research in BOTDA sensors has been directed towards developing methods to improve their performance in terms of spatial resolution, sensing range and measurement time, as well as simplifying the deployed setups to reduce the cost of the sensor. However, this technology is quickly reaching maturity and latest research on BOTDA sensors is increasingly focused on analyzing the fundamental factors that determine their ultimate performance.

One of the most fundamental limitations in a BOTDA comes from the optical power of the pump and probe waves that can be injected into the sensing fiber, because this defines the signal-to-noise ratio (SNR) of the detected sensor response, which is the quantity that ultimately constrains the performance of the sensor [1]. The maximum pump pulse power that can be introduced in the fiber is limited by the onset of modulation instability (MI) [2] or self-phase modulation (SPM) [3]. Whereas the maximum probe power that can be deployed is also limited, because, for large power, the energy exchanged between the pump and probe waves through Brillouin interaction becomes significant, so that the pump pulse becomes depleted as it propagates along the fiber. This leads to so-called non-local effects, because the Brillouin spectra measured at distant locations depend on the interaction at previous positions in the fiber. Moreover, the pump depletion has a dependence with the frequency difference between pump and probe waves, hence, leading to errors in the measurement of the Brillouin frequency shift (BFS) [4].

We focus here on another limiting factor for BOTDA sensors that has been largely overlooked to date: the pedestal of the pump pulses deployed in the sensor [5]. Any practical device that is used to generate the pump pulse is bound to have a limited extinction ratio (ER). Therefore, in addition to the pulse, there is a CW pump power, the pulse pedestal, that leaks through the pulsing device and counter-propagates with the probe wave along the fiber, leading to an extra amplification of the latter. In the literature, there are few references to the deleterious effects of the finite ER of the pump pulses. In an early work, our group showed that the extra amplification of the probe wave by the pump pedestal could lead to an exacerbation of the pump pulse depletion and non-local effects [6]. Another negative impact of limited ER pump pulses comes from the worsening of the SNR of the sensor due to laser phase noise [7]. In addition, a rather conservative and somewhat arbitrary requirement on the ER of the pulses in a BOTDA sensor was established

in the context of the modeling of non-local effects due to pump depletion [4]. This requirement stated that the ER should be sufficient to guarantee that the Brillouin amplification of the probe provided by the pedestal of the pulse along the full sensing length had to be smaller than the local amplification by the pulse itself. This translates to the condition that the lower bound for the ER must be  $ER > L_{eff}/u$ , where  $L_{eff}$  is the effective fiber length, which tends asymptotically to  $L_{eff} \approx 22$  km for typical long-length fibers, and  $u$  is the spatial resolution of the BOTDA sensor. For instance, according to this condition, an ER larger than 43 dB would be necessary for 1-meter spatial resolution measurements in long-range BOTDAs. Such a large ER is typically just within the reach of semiconductor optical amplifier (SOA) switches or acousto-optic modulators (AOMs). However, these pulse shaping devices have rise and fall times that are typically of the order of 1 ns for SOAs and longer for AOMs, which compromise the capability to perform high-spatial-resolution measurements using, for instance, the differential pulse-width pair (DPP) technique [8]. Furthermore, pulses with less steep leading and trailing edges are prone to the deleterious effects of SPM, which has been shown to degrade BOTDA performance [3]. In order to generate the sharp pulses that are needed for high-spatial-resolution measurements using DPP, a Mach-Zehnder electro-optic modulator (MZ-EOM) is required. However, MZ-EOMs usually have a low ER, typically of the order of 20 to 30 dB, which would not comply with the rigid conservative condition for the ER stated above. Note that two cascaded MZ-EOMs could be used in order to keep the fast response with an improved ER, but at the expense of an added setup complexity and an increased cost of the sensor.

Therefore, it is necessary to study in further detail the constrains imposed by the ER of the pump pulses, which is precisely what we do in this paper with the help of a new theoretical model that is used for numerical calculations of the interactions between the various waves involved in the BOTDA sensor. As a result of this analysis, we have identified two previously unknown detrimental effects imposed by low ER pump pulses on BOTDA systems. The first one originates in the increased depletion of the pedestal following the pump pulse by the amplified probe wave. This is found to introduce a non-local effect which has analogous impact to non-local effects originated in the pulse depletion. The other closely-related effect found is due to the transient response of the erbium-doped fiber amplifiers (EDFA) that are usually deployed to amplify the pump pulse before injection into the sensing fiber. The EDFA amplification distorts the pedestal that follows the pulse and this again induces a non-local effect that impairs the measurements. In the following, both effects are studied theoretically, through numerical calculations, and experimentally.

## 2. Theoretical model for pump and probe waves interaction

As it is well-known, in a BOTDA sensor two counter-propagating waves interact via stimulated Brillouin scattering in a single-mode fiber: a pulsed pump wave and a CW probe. We are concern here with a scenario in which the pump pulse that is launched into the fiber has a limited ER and, hence, it is on top of a CW pedestal. This interaction can always be solved by using the full time-depend coupled equations for the amplitudes of the pump and probe optical fields and the acoustic wave [9]. However, this would be computationally intensive, particularly for the long-range BOTDA sensors that are considered in this research. Therefore, we introduce here a new simplified model that is going to be used to analyze the effects of the pump pulse ER upon the performance of BOTDA sensors. This model will be validated by the experiments in sections 5 and 6.

The model assumes that the pulses are longer than the acoustic phonon lifetime so that a perturbation method can be used to solve the steady-state coupled power equations for the

Brillouin interaction between pump and probe waves along the fiber:

$$\frac{d}{dz}P_S(z) = -\frac{g_B(\nu, z)}{A_{eff}}P_S(z)P_P(z) + \alpha P_S(z) \tag{1a}$$

$$\frac{d}{dz}P_P(z) = -\frac{g_B(\nu, z)}{A_{eff}}P_S(z)P_P(z) - \alpha P_P(z) \tag{1b}$$

where  $P_S$  and  $P_P$  are the optical powers of probe and pump wave respectively, at each position  $z$  of the fiber,  $\alpha$  is the attenuation coefficient,  $A_{eff}$  is the effective area and  $g_B(\nu, z)$  is the Brillouin gain coefficient of the fiber, which depends on the frequency shift between pump and probe waves at each position.

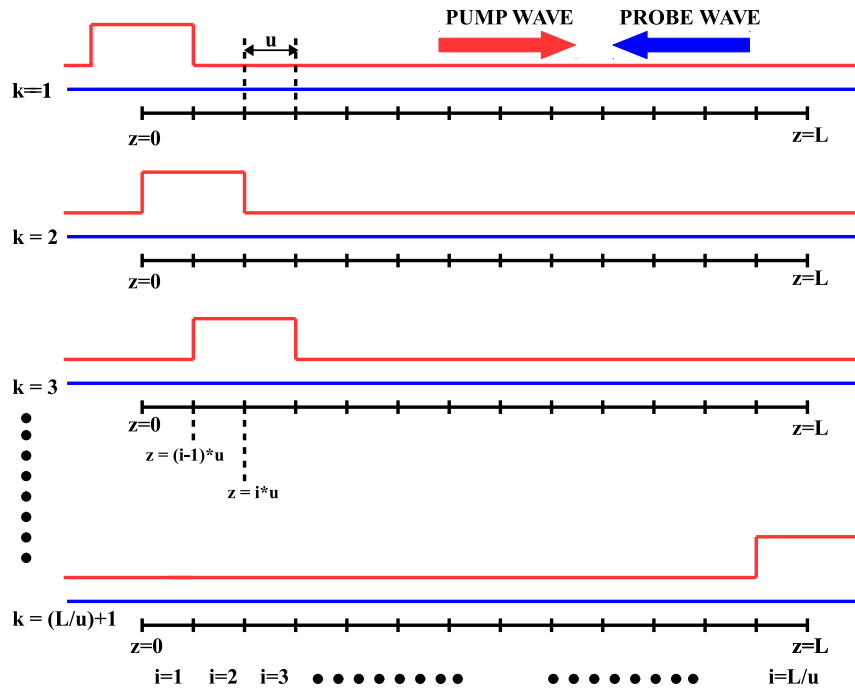


Fig. 1. Fundamentals of the theoretical model. The fiber is divided into segments equal to the spatial resolution and the interaction between pump and probe is solved for each segment  $i$ . The waves are then counter-propagated in successive iterations.

As it is highlighted in Fig. 1, the fiber is first divided into segments of length  $u$  equal to the spatial resolution of the sensor, i.e., half the spatial width of the pump pulse in the fiber. Then, in order to calculate the evolving powers of the counter-propagation of pump and probe signals, successive iterations are carried out. At each iteration  $k$ , the interaction between pump and probe wave is calculated in all the  $N = L/u$  segments in which the fiber has been divided, with  $L$  the total fiber length. This is done by solving (1) for each segment,  $i$ , from  $i = 1$  to  $i = N$ , using the

boundary values of the pump and probe wave powers. This gives:

$$P_S((i-1)u) = P_S(iu) \exp\left(\frac{g_B(v, z)}{A_{eff}} P_P((i-1)u) u\right) \exp(-\alpha u) \quad (2a)$$

$$P_P(iu) = P_P((i-1)u) \exp\left(-\frac{g_B(v, z)}{A_{eff}} P_S((i-1)u) u\right) \exp(-\alpha u) \quad (2b)$$

where (2a) gives the amplified probe wave by approximating the pump power as constant along the  $i$ -th segment, from  $z = (i-1)u$  to  $z = iu$ , and equal to the power at the input of the segment,  $P_P((i-1)u)$ ; hence, neglecting the pulse depletion induced by the probe wave for this calculation. Similarly, (2b) is solved by approximating the probe wave to be constant in the segment. Note that the pump and probe interaction is calculated identically in every segment regardless of whether it is a pulse-probe or a pedestal-probe interaction.

Then, for the next iteration,  $k+1$ , all probe and pump waves calculated in the previous iteration are advanced one step of length  $u$  in opposite directions and again the interactions are recalculated in all  $i = 1$  to  $i = N$  segments. The process continues until the pulse has left and the probe wave from the farthest location of the fiber has had time to traverse the fiber and leave. Typically, the iterations are continued even longer in order to see effects that are due to the propagation of the pedestal following the pulse, the trailing pedestal, which will be highlighted in section 3. Note that before beginning the interaction between pump and probe waves, all segments of the fiber are filled with the corresponding pump and probe waves values taking only into consideration the attenuation of the fiber. Moreover, it is necessary to start the iterations before the arrival of the pulse to the input of the fiber so that the initial interaction between the probe wave and the pedestal of the pump that precedes the pulse, the leading pedestal, have time to converge. For this reason, the total number of iterations is typically an order of magnitude larger than  $l = 2L/u$ , which are the minimum iterations to fully propagate the pulse and the amplified probe.

This model can be regarded as an enhancement of previous perturbation methods for solving the waves interaction in BOTDA sensors [6, 10]. Notice, that the model can be applied to BOTDA sensors in either gain or loss configuration. Furthermore, it can be also applied to dual-probe setups simply by adding in (1) the terms corresponding to the additional probe wave component [11].

### 3. Extinction ratio effects in BOTDA

The previously presented model is deployed in this section to perform an analysis of the impairments brought by the limited ER of the pump wave in BOTDA sensors. All the presented calculations assume typical standard single-mode fiber (SMF) parameters for the Brillouin interaction:  $g_B = 2 \times 10^{-11}$  m/W,  $A_{eff} = 80 \times 10^{-12}$  m<sup>2</sup>,  $\alpha = 0.2$  dB/km and Brillouin linewidth of 30 MHz. The use of a scrambler or polarization switch to compensate polarization induced variations of the Brillouin gain is also taken into account, which entails a reduction factor of 1/2 in the induced Brillouin gain [12].

The section is organized as follows. First, the worsening of pump pulse depletion due to the additional probe wave amplification by the leading pedestal of the pulse is described. This is an extension to dual-probe BOTDA sensors of a previous study that was limited to conventional single-probe BOTDA setups [6]. Then, two completely new impairments brought by the limited ER of the pump pulse are introduced: a measurement distortion caused by the depletion of the trailing pedestal, and another distortion generated by the interplay between the pulse pedestal and the transient behavior of the EDFAs that are typically deployed to increase the pump power injected into the FUT.

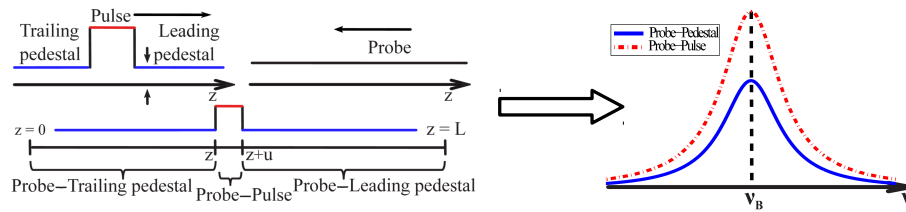


Fig. 2. Schematic description of probe and pulse wave interaction along the fiber and its consequences in the measured Brillouin gain spectrum (BGS).

### 3.1. Pump pulse depletion increase induced by the pedestal of the pump wave

Figure 2 schematically depicts the three regions of interaction with the pump wave that a probe wavefront finds as it travels along the fiber. The first region extends from the probe wavefront entrance in the fiber at  $z = L$  to the location of the pulse at a particular  $z = z_0 + u$ . In this region, just the leading pedestal of the pump pulse and the probe wave interact, leading to Brillouin amplification of the probe wave. Then, the probe wavefront meets the pulse and is amplified over a length  $u$  of fiber equal to half the spatial width of the pulse in the fiber (spatial resolution). Finally, after leaving the pulse location, there is another interaction region, from  $z = z_0$  to  $z = 0$ , where the probe wave is again amplified by the pump wave trailing pedestal.

Therefore, the net effect of the presence of the pump wave pedestal is that the probe wave experiences more gain than just that due to the pulse itself. Moreover, this is a gain that is not useful for sensing. On the contrary, as it is shown on the right of Fig. 2, it manifests as a Lorentzian gain spectrum that appears due the probe and pulse pedestal interaction, in addition to the gain spectrum induced by the pulse itself. In principle, the latter can be recovered by normalizing the measurements by the spectrum measured with no pulse in the fiber, i.e., subtracting the gain experienced by the probe due to interaction with just the pedestal before the pulse enters the fiber from the total measured gain. In fact, the additional gain in the probe wave has been shown to degrade the precision of the BFS measurement [6]. Moreover, the presence of this additional gain, apart from the useful signal, can lead to an effective reduction of the SNR because the full-scale dynamic range of the analog-to-digital converter within the signal acquisition device is largely wasted with a detected signal larger than the signal of interest; hence increasing the quantization noise.

In addition, the extra amplification of the probe wave by the leading pedestal of the pulse aggravates the depletion of the pulse as it propagates along the fiber since it meets a higher power probe wave and more energy is transferred from the pulse to the probe. This leads to a worsening of non-local effects [6]. We focus here on a dual-probe wave BOTDA configuration, where this effect has not been previously studied. In this case, the interaction with the leading pedestal of the pulse from  $z = L$  to  $z = z_0 + u$  unbalances the power of the two probe waves: the upper optical frequency probe is attenuated and the lower frequency probe is amplified. This, in turn, leads to an unbalance of the gain and loss spectra that both waves induce upon the pulse: the gain induced by the higher frequency probe is reduced and the loss induced by the lower frequency probe is increased. Hence, they no longer compensate each other leading to pulse depletion. Note that this depletion is, at equal probe power levels, smaller than that in a conventional single-probe BOTDA.

Figure 3 depicts the calculated depletion spectrum experienced by the pump pulse in an uniform BFS fiber link for different ER values, by portraying the depletion factor of the pump pulse as a function of the frequency detuning of the pump and probe waves [4]. The probe wave power was set to -3 dBm per sideband, which is the maximum power that can be deployed in a long-range dual-probe sideband BOTDA sensor before the appearance of second-order non-local effects [13].

A 10-ns pump pulse was assumed with a peak power of 20 dBm, which is typically the largest pulse power that can be injected in a long-range fiber link before the onset of MI [2]. Finally, a 25-km length of fiber was chosen as a representative long-range link larger than the typical effective length for non-local effects ( $L_{eff} \approx 1/\alpha$ ). This figure highlights that the depletion factor increases considerably for decreasing ER of the pump pulse. Notice that the tolerable maximum depletion factor for a given error is reached at lower probe wave power. For instance, the approx. 20%-depletion that can be tolerated for around 1-MHz BFS measurement error [4]. Thus, the maximum probe power that can be injected in the sensing fiber decreases with the pump wave ER, which leads to a worse SNR and, consequently, to a reduction of the accuracy of the sensor.

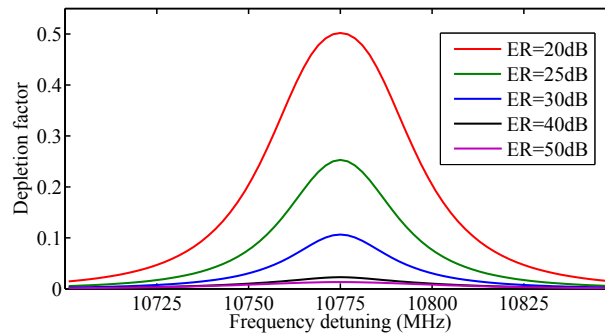


Fig. 3. Resultant depletion factor,  $d$ , of the pump pulses as a function of their ER in a long-range BOTDA sensor.

The worsening of the pulse depletion with decreasing ER is not going to be analyzed further here as this effect does not take place isolated. It is accompanied by a new effect that has been found in this work, which is due to the depletion of the pulse pedestal.

### 3.2. Non-local effects due to pump wave pedestal depletion

Apart from the increased pump pulse depletion, there is another effect, which has not been previously described, that also distorts the measurements in BOTDA sensors with limited ER of the pump pulses. Figure 4(a) depicts several calculated BOTDA traces, i.e. the gain provided by the pulse to the probe wave as a function of position along the fiber, for the system considered in the previous subsection (same conditions than in Fig. 3) as a function of the ER of the pump pulse. These traces are for a frequency separation between pump and probe waves equal to the BFS of the fiber, i.e., peak Brillouin interaction. As it can be observed, there is a distortion of the shape of the measured probe wave signal for decreasing ER of the pump pulse.

In order to explain the origin of the distortion observed in Fig. 4(a), it is necessary to complete the scenario outlined in Fig. 2 and discussed above. Let's consider first the conventional single-probe BOTDA case. Previously, we described how the pump pulse meets a probe wavefront at a particular  $z = z_0 + u$  that had been amplified by interaction with the leading pedestal of the pump pulse in the  $z = L$  to  $z = z_0 + u$  region, and how it makes the pump pulse experience an increased depletion. Now, we focus on the trailing pedestal of the pulse, which meets a probe wavefront that has been amplified by the pulse. Hence, in the interaction region from  $z = z_0$  to  $z = 0$ , the trailing pedestal experiences an increased depletion, because more energy is transferred from the pedestal of the pump wave to the higher power probe. Moreover, the increased depletion of the trailing pedestal leads to a reduced amplification of the probe wave in its final journey to the exit of the fiber.

In order to understand the consequences of this reduced amplification of the probe wavefront by the trailing pedestal, it is necessary to remember that the normalized BOTDA trace is obtained by subtracting the gain measured when there is no pulse, i.e. before the input of the pulse, in the

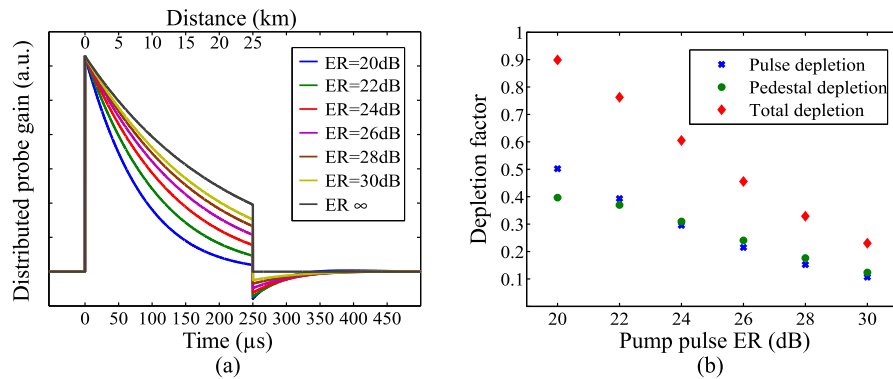


Fig. 4. (a) Brillouin gain of the probe wave. The traces are depicted in terms of time-of-flight of the pump pulse with an added axis (top) with the translation to location along the fiber. (b) Values of pulse depletion factor,  $d$ , pedestal depletion factor,  $d_P$  and total depletion factor,  $d_T$ .

fiber from the total measured gain which, as it has been explained, includes contributions from the pump pulse and its pedestal. If there were not increased depletion of the trailing pedestal of the pulse, the gain measured without pulse would be just the part of the measured gain due to the pedestal, and, hence, this normalization operation would give the correct probe gain due to just the interaction with the pulse. However, that is not the case: due to the reduced amplification of the probe in its interaction with the trailing pedestal, the gain measured without pulse is actually larger than the portion of probe gain due to the pedestal. Furthermore, the difference becomes larger as we consider locations  $z = z_0$  in the fiber that are closer to the entrance of the probe at  $z = L$  because then the interaction region between the probe wavefront and the trailing pedestal of the pulse is larger.

In the case of a dual-probe BOTDA sensor the explanation of the effect is similar. As it was explained before, the two probe waves power unbalance as they interact with the leading pedestal of the pulse from  $z = L$  to  $z = z_0 + u$ . The interaction with the pulse further unbalances the powers of the two-probe wavefront; hence the trailing pedestal of the pulse is further depleted and the gain of the lower-frequency probe in its journey to the exit of the fiber is reduced. As before, this effect of reduced amplification of the probe, at equal power levels, is smaller in a dual-probe BOTDA than in a single-probe setup. If instead of the lower-frequency probe, we keep the loss of upper-frequency probe for sensing, the effect is identical, but this time it translates into a reduced loss of the upper-frequency probe in its interaction with the trailing pedestal of the pulse.

The explanations above justify the shape of the BOTDA traces in Fig. 4(a). For locations close to the pulse entrance at  $z = 0$  the measured gain is largely independent of the ER of the pulse. For these locations the length of the region of interaction between the probe wavefront and the trailing pedestal of the pump pulse is nonexistent or very small; hence, the gain without pulse in the fiber is similar to the gain provided by the pedestal to the probe, and the normalization works well. However, as the pulse advances along the fiber, the interaction region between probe and trailing pedestal becomes larger and hence the use of the gain without pulse for normalization of the trace overestimates the pedestal contribution, which leads to a progressive reduction of the trace amplitude. The effect is more pronounced for smaller ER of the pulse.

Furthermore, it can be seen that even after the pulse has left the fiber (at  $L = 25$  km), there is still a signal feature which depicts an abrupt fall to negative normalized gains followed by a slow recovery. The existence of this feature is due to the fact that the probe wavefronts that enter the fiber after the pulse has exited, do still interact with a trailing pedestal of the pulse that has been depleted by all the previous probe wavefronts that it has met during its journey through the fiber.



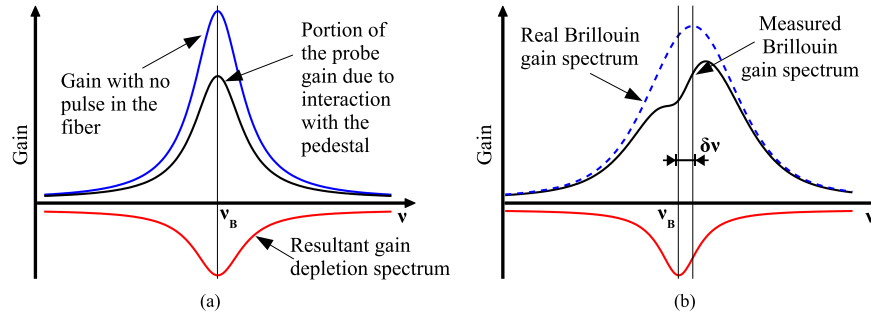


Fig. 5. (a) BOTDA gain depletion spectrum induced by the different spectra used in the measurement normalization process. (b) Distortion of the measured spectrum due to gain depletion.

The distortion due to non-local effects induced by the pump pedestal depletion leads to errors of the measured BFS. Figure 5(a) schematically depicts the frequency dependence of the distortion induced by the depletion of the trailing pedestal of the pulse assuming a fiber with uniform BFS. The spectrum of the probe gain measured with no pulse in the fiber is displayed together with the calculated spectrum for the portion of the probe gain that comes from interaction with the pedestal at a particular position in the fiber. It can be seen that the net effect of the trailing pedestal depletion is the introduction of an additional Lorentzian loss transfer function when the resultant spectrum of the probe gain without pulse in the fiber is used for normalization, instead of the smaller real spectrum of the gain due to interaction of the probe with the pedestal. As it is shown in Fig. 5(b), if we assume a worst-case scenario in which a length of uniform BFS fiber is followed by a small section at the end with a different BFS, e.g. a hotspot, a distortion is introduced in the measured gain spectrum due to the additional transfer function added by the probe gain depletion induced by the trailing pedestal depletion. This is completely analogous to the effect of pump pulse depletion that gives rise to non-local effects [4]. In fact, this is a new form of non-local effect but originated in the pedestal depletion when low ER pulses are deployed. This effect can be characterized by a dimensionless factor  $d_P$ , which we call pedestal gain depletion factor, that depends on the position  $z$  of the fiber and that is given by:

$$d_P = \frac{G_P - G'_P}{G_P} \quad (3)$$

where  $G'_P$  is the portion of the probe gain that comes from the pedestal and  $G_P$  is the probe gain with no pulse in the fiber. This coefficient can be used in an identical manner to the pulse depletion coefficient to derive the BFS measurement error induced by this new non-local effect [4]. Therefore, the BFS error induced by this pedestal depletion effect reaches its maximum in a worst-case scenario in which a constant BFS fiber has a small segment at its end with a BFS that is separated by that of the rest of the fiber by approximately 1/4 of the Brillouin spectral width [4].

Note that the pedestal-induced non-local effects take place simultaneously to those induced by the pump pulse depletion. Altogether, the BFS measurement errors in a BOTDA sensor are given by the total amount of depletion of the BOTDA trace,  $d_T$ , which comes from the addition of  $d$  and  $d_P$  factors.

$$d_T(\nu, z) = d(\nu, z) + d_P(\nu, z) \quad (4)$$

In fact, in Fig. 4(a) there is some trace amplitude reduction that is due to the increased pump pulse depletion for limited ER pulses that was described in subsection 3.1. Note that the depletion

factor  $d$  implies an analogous reduction of the Brillouin gain of the probe wave. Figure 4(b) depicts the different components of the total depletion factor at the end of the fiber as a function of the ER of the pulse. It can be seen that the depletion factor due to the pedestal depletion has a similar influence than the depletion factor of the pulse.

The theoretical model that we have developed in this work (section 2) can be used to derive guidelines for the design of BOTDA systems. Figure 6(a) depicts the calculated values for the maximum probe wave power that can be used in a long-range dual-probe BOTDA sensor to obtain a maximum error of 1-MHz in the determination of the BFS. The results are given as a function of the ER of the pump pulses deployed. This figure has been calculated by finding the maximum probe wave power that lets to  $d_T \approx 0.2$  [4]. It can be observed that decreasing the ER of the pump pulse wave translates to a more restrictive power limit for the probe wave. In addition, it can be seen that in order to be able to inject in the fiber a probe power of -3 dBm per sideband, which is the limit for the onset of significant second-order non-local effects [13], an ER higher than 32 dB would be necessary. Note that this is above the ER than conventional electro-optic modulators provide, which typically lies between 25 and 30 dB. Furthermore, if a technique for mitigation of second order non-local effects was deployed [14], then the probe power would be limited to around 6 dBm due to the Brillouin threshold of the fiber [15]. According to Fig. 6(a), this would require an ER greater than 43 dB. Curiously, in this case, the calculated ER limit coincide with the somewhat arbitrary  $ER > L_{eff}/u$  condition stated in previous studies [4]. However, for lower probe powers, that condition is rather conservative.

The maximum probe wave in Fig. 6(a) was calculated for the worst-case length of the fiber link that leads to maximum  $d_T$ . Figure 6(b) depicts which was that worst-case length as a function of the ER of the pump pulse. It can be observed that for large ER the worst-case length tend to  $L = 1/\alpha$ , which is consistent with previous studies of non-local effects that consider the ER to be infinite [4]. However, for lower ER the worst-case length of the link becomes larger. Finally, Fig. 6(c) depicts, for each ER in Fig. 6(a) and 6(b), which was the relative contribution of  $d$  and  $d_P$ . As can be seen, the contribution to the total depletion given by pedestal depletion is greater for  $ER \leq 35$  dB. Whereas for larger ER the contribution of pulse depletion is higher. In addition, it can be observed that for pump pulses of an ER up to 40 dB both depletion effects have a significant contribution.

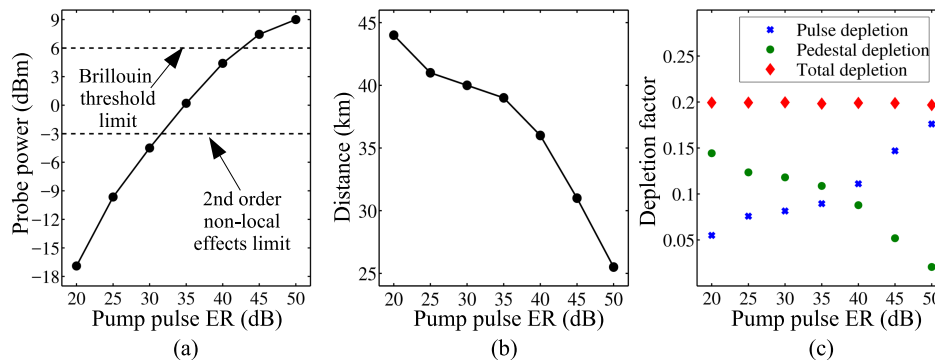


Fig. 6. For a maximum tolerable 1-MHz error in BOTDA measurement with a pump pulse of 20 dBm peak power and 10 ns duration: (a) maximum probe wave power per-sideband that can be deployed, (b) length of the sensing fiber where the total depletion factor reaches its maximum value and (c) depletion factor  $d$ ,  $d_P$  and  $d_T$  in these conditions.

Finally, it should be pointed out that the theoretical model for the non-local effect induced by the pedestal depletion can be used to study the dependencies of this effect on system parameters. It has been found that the effect increases with increasing power of either probe or pump wave.

Therefore, the calculations in this section, which have been performed for the highest practical powers of these two waves, constitute a realistic scenario. Moreover, the effect has been found to have a very small dependence with the pulse duration, considering that the measurement distortion is proportional to the Brillouin gain induced by the pulse. A detailed analysis of these dependencies is outside the scope of this work and will be reported elsewhere.

### 3.3. Effects of the transient response of EDFAs in BOTDA sensors

In this work, we have also found another new measurement distortion effect in BOTDA sensors, which is induced by the interplay between the transient behavior of the EDFA and the pedestal of low-ER pulses. It is well known that EDFAs present a transient behavior when amplifying pulsed signals that is due to the long recovery time of the population inversion of the erbium ions after amplifying an optical pulse [16, 17]. In BOTDA sensors with low ER pulses, this effect distorts the pump pulse shape because the EDFA has a different instantaneous gain before the arrival of the pulse, i.e. for the leading pedestal, than for the trailing pedestal. The pulse arrival depletes the population inversion in the EDFA so that the trailing pedestal initially experiences less amplification than it should. This amplification slowly recovers but a permanent distortion of the trailing pedestal is induced.

The effects of the distortion of pump pulse pedestal induced by EDFA response are similar to those originated by the trailing pedestal depletion that were described in the previous section. The contribution to the measured gain of the probe wave is smaller for the interaction with the distorted trailing pedestal than with the leading pedestal. Hence, again, the use of the probe gain without pulse in the fiber to normalize the measurements induces an error, because the portion of the gain due to interaction with the pedestal becomes overestimated. This leads to an independent and additional depletion factor, which is induced by the EDFA transient response.

Due to the fact that the transient gain response of an EDFA for the pulse amplification depends on the EDFA design itself, the development of a theoretical analysis of this effect is complicated. Moreover, this transient response displays a complex dependence on the pulse power, duration, etc. [17]. Therefore, as the behavior of EDFAs can not be generalized, we will study the details of this effect after its experimental demonstration in section 6 of the paper.

## 4. Experimental setup

Figure 7 depicts the dual-probe BOTDA setup that was deployed to experimentally demonstrate the effects of the limited ER of the pump pulses on BOTDA sensors and also to validate the theoretical model presented above. The optical source was a 1560-nm distributed feedback laser, whose output was divided by a coupler into two branches. In the upper branch, the pump pulse wave with tunable ER was generated by using either a MZ-EOM or a SOA switch. The SOA was

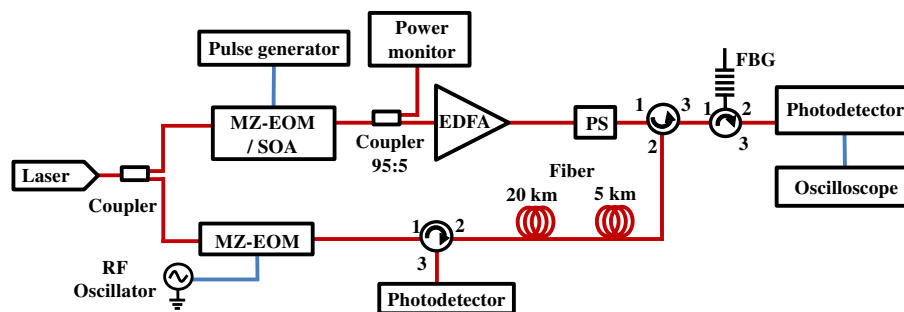


Fig. 7. Experimental setup deployed to demonstrate the effects of the pump pulse ER on BOTDA sensors.

deployed to provide pulses with a high ER of around 45 dB. The MZ-EOM was used to generate pulses with ER from 20 to 26 dB by adjusting its bias point and the amplitude of the electrical pulsed signal driving the device. The pump pulsed signal was then amplified with an EDFA, filtered to reduce the amplified spontaneous emission (ASE), and directed to a polarization scrambler before injecting it to the FUT. The pump peak power was limited to 20-dBm in order to avoid MI effects in the fiber. Moreover, in most of the measurements the pump pulse duration was set to 60-ns in order to have a good SNR, particularly in measurements that used very small probe power.

The pump pulse signal was counter-propagated along the FUT with a double-sideband suppressed-carrier probe wave, which was generated in the lower branch of the setup using another MZ-EOM driven by a radio-frequency generator tuned to the BFS of the fiber and biased for minimum transmission. Finally, a tunable narrow-band fiber Bragg grating (FBG) was used to filter out one of the probe sidebands before using a receiver to detect the signal with an oscilloscope. At the other end of the FUT, the depletion of the pump pulses was monitored using a circulator and another detector.

The FUT was comprised of two different fiber spools with 5-km and 20-km length and same BFS but slightly different Brillouin gain coefficient. In addition, two hotspots were prepared along the FUT using a climatic chamber: one after the first spool and the other at the end of the link.

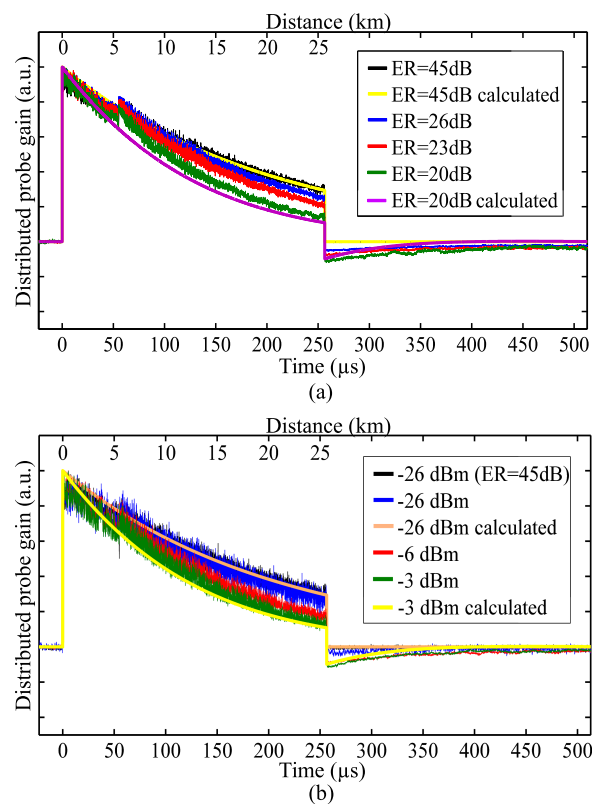


Fig. 8. BOTDA trace distortion due to the ER of the pump pulse. (a) Dependence on the ER level; (b) Dependence on the probe wave power for a fixed ER of 23 dB. The black line shows the same for an ER of 45 dB, for comparison.

## 5. Demonstration of non-local effects due to pump pulse limited ER

Experiments were performed to experimentally demonstrate the non-local effects originated by the limited ER of pump pulses in BOTDA sensors. In order to avoid effects due to the EDFA transient response, an EDFA (Amonics Ltd. Pulsed EDFA) specially designed for amplification of isolated pulses with almost no distortion was deployed in these experiments. Figure 8(a) shows the detected BOTDA traces measured at the maximum BFS of the fiber when pump pulses with different ER were counter-propagated to a -3-dBm dual-probe wave. Notice that, the BOTDA trace detected using the SOA is the only one that suffers no distortion, while the traces obtained using the EOM are distorted by the interaction between the probe waves and the pump wave trailing pedestal. As it can be observed, the BOTDA trace distortion increases when the ER is worsened. The figure also shows the traces calculated using the theoretical model introduced in 2, which agree well with the experimental results. The small deviation between theory and experiments is attributed to the residual effects of the EDFA transient response that will be analyzed later.

Figure 8(b) also depicts BOTDA traces, but this time measured for a fixed ER of the pump pulses of 23 dB and with different probe power levels. For comparison the black line shows an ER of 45 dB, obtained with a SOA switch and a low probe wave power. As it was expected, the distortion of the traces increases for increasing probe power. For low probe power the measured signal matches that obtained with the large ER SOA switch. However, as the probe power is risen, it starts to deplete the trailing pedestal of the pulse and hence the trace amplitude is reduced by the normalization performed, as it was previously explained, leading to the appearance of the newly described non-local effects. Again, in this figure, the calculated theoretical values are also shown to agree well with the experiments.

Figure 9 depicts the measured depletion factors at the end of the fiber link as a function of the probe power. Pulse depletion, pedestal depletion and total depletion factors are represented. The obtained results are plotted together with the theoretical calculations performed using the theoretical model. Note that the theoretical calculation of the pedestal gain depletion is presented with and without taking into account the EDFA transient effects that will be studied in the next section. These effects are shown to introduce an additional depletion factor, even though the deployed EDFA in these experiments had very small transients. Notwithstanding, there was a good general agreement between the experimental results and the model calculations. This figure demonstrates that the non-local effect due to the pedestal depletion in limited-ER BOTDA sensors are very significant, contributing in the same order of magnitude than the effects due to the pump pulse depletion.

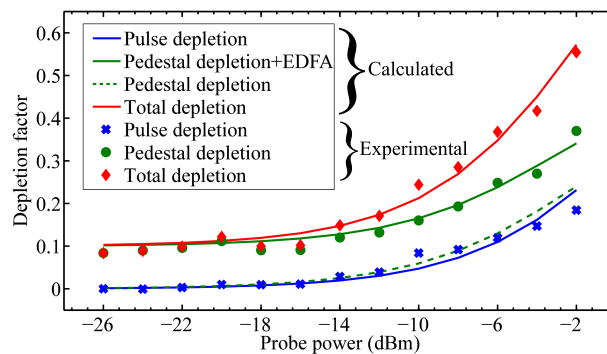


Fig. 9. Depletion factor  $d_p$  and  $d$  dependence on the probe wave power when deploying pump pulses with 23-dB ER.

Finally, the BFS error introduced by the effects of the ER of the pump pulses was characterized. For this purpose, the Brillouin gain spectrum was measured along the fiber while the temperature of the hotspots was fixed by a climatic chamber at 9° C of difference from the rest of the fiber, which was also controlled by another climatic chamber. The resultant BFS distribution along the 2 hotspots are depicted in Fig. 10. As it is observed, the error with respect to the reference measurement performed with the SOA is worsened with increasing the fiber distance, as it was expected. So there is negligible error in the first hotspot, whereas, for the second hotspot at the end of the fiber, the BFS error becomes significant. In addition, the effect increases when the ER is worsened, so that at hotspot at the end of the fiber the BFS error raises to 3, 4.5 and 7.5 MHz for 25, 23 and 21 dB ER pulses, respectively. Note that as the temperature of the hotspot was heated the BFS is overestimated, while if the fiber at the hotspot had been cooled the BFS would be underestimated, as with other non-local effects.

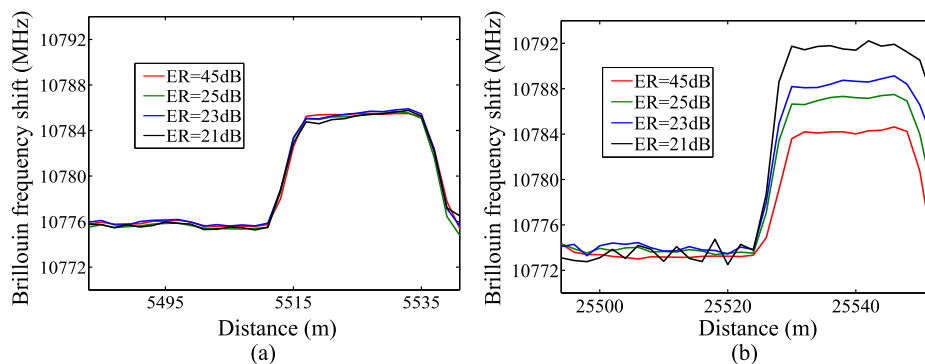


Fig. 10. Measurement error induced by 25-dB, 23-dB and 21-dB ER pump wave in different positions of the fiber for a -3 dBm per sideband probe wave power: (a) at a distance of 5 km and (b) at the end of the fiber.

## 6. EDFA transient response characterization and influence on BOTDA sensors

The other measurement distortion effect that was experimentally investigated was due to the interplay between the transient response of EDFAs and the limited ER of the pump pulses in BOTDA sensors. First, a detailed characterization of the transient responses of several EDFAs was performed, and then their distortion effects on BOTDA measurements were assessed.

The transient response of an EDFA while amplifying a pulse can not be simply measured by monitoring its time-domain output power because the dynamic range required to be able to observe simultaneously the pulse and the small effects on the pulse pedestal is too large. Therefore, we devised the experimental setup depicted in Fig. 11, which is based on adding an extra CW signal generated by another laser to the pump pulse signal to be amplified so that the transient variations of the EDFA gain could be monitored on this signal. The extra laser signal was separated by 0.5 nm from the pulse wavelength and its power was set to be 10-dB lower than the average power of the pump wave so that its addition had a negligible effect on the EDFA transient response. At the output of the EDFA the monitoring wavelength was separated with a FBG and detected in a photo-receiver followed by an oscilloscope, where the precise variations of the gain of the EDFA while amplifying the pump wave could be measured.

Three commercial EDFAs set for a nominal 20-dB gain were tested to compare their performances: EDFA I (MPB Communications Inc.), has 3 amplifying stages and 21-dBm saturation power, EDFA II (Manlight S.A.S) provides 23-dBm output saturation power using 2 pump stages and EDFA III (Amonics Ltd. Pulsed EDFA) corresponds to the special amplifier design for pulse

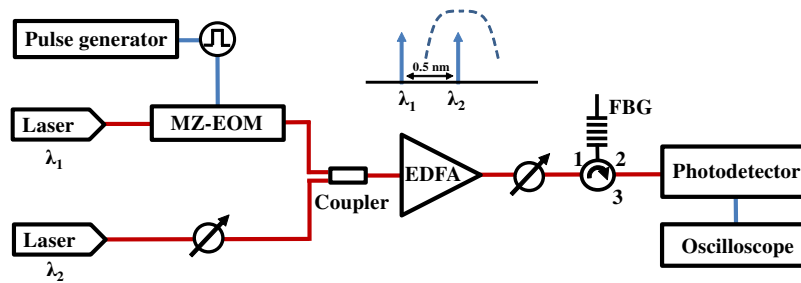


Fig. 11. Experimental setup deployed for the characterization of the EDFA transient responses to pulsed signal amplification.

amplification deployed in section 5. Figure 12 shows the temporal variation of the gain of the three EDFAs when they amplify the pump pulsed signals with different ER (20, 23 and 26 dB). Notice that the arrival of the pulse perturbs the gain of EDFA I and II, which display a transient response after the pulse amplification. EDFA I has a larger variation of the gain than EDFA II, however, the recovery time is longer for the latter. The magnitude of the transient variation of the gain depends on the ER of the pulses. For the two EDFAs, the greater the ER, the larger the gain change. In contrast to EDFAs I and II, EDFA III displays a smaller variation as expected.

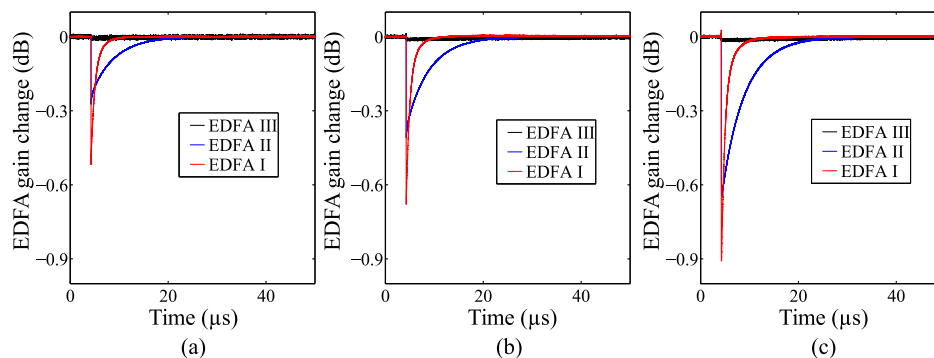


Fig. 12. Variation of the EDFA gain after the amplification of pump pulses with ER of (a) 20 dB, (b) 23 dB and (c) 26 dB. Three different commercial EDFA are measured.

Figure 13(a) and 13(b) show the BOTDA trace distortion when EDFA I and EDFA II were deployed to amplify the pump wave with different ER levels, 20 dB, 23 dB, 26 dB and 45 dB. The probe wave sidebands were set to -18.5-dBm power to ensure that non-local effects either due to pump pulse or pedestal depletion were negligible. When a 45-dB ER SOA is deployed to shape the pump pulses, the BOTDA traces remain undistorted for the two amplifiers, with just the characteristic 0.2 dB/km roll-off of the fiber loss coefficient. In this case, the transient response of the EDFA has no effect since the pedestal of the pulse is negligible. On the contrary, the use of a limited ER EOM leads to severe distortion of the measurements. The smaller the ER, the larger the distortion. Moreover, it was found that the distortion does not depend on the probe power. Calculations using the model introduced in section 2 are also plotted in the figure, showing excellent agreement with the experimental results. This calculation used a pump wave signal incorporating the trailing pedestal distortion measured in Fig. 12.

The origin of this BOTDA measurements distortion lies in the variation of EDFA gain after the pulse that was depicted in Fig. 12. This variation changes the shape of the trailing pedestal of the

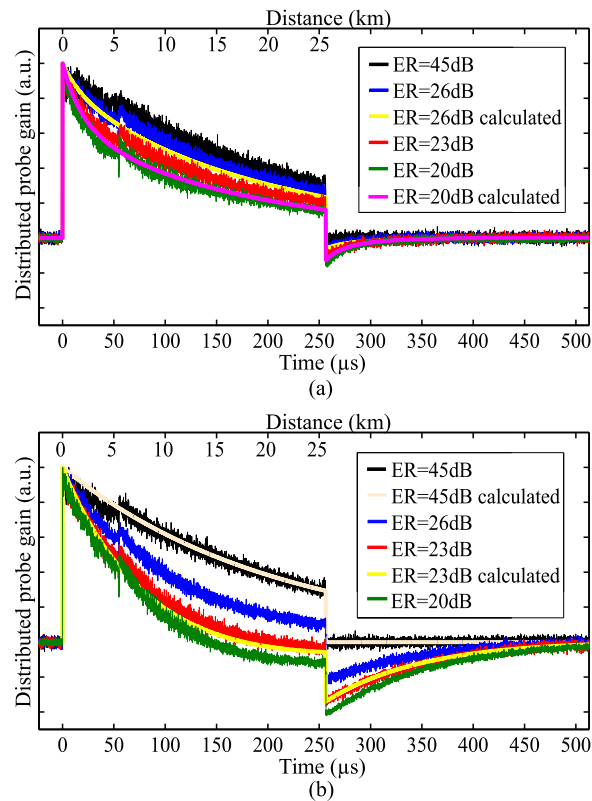


Fig. 13. Experimental and theoretical BOTDA trace distortion due to EDFA transient response for different pump pulse ER values and different EDFA, (a) for EDFA I and (b) EDFA II.

pump pulse so that its amplitude is initially reduced and then recovers. Subsequently, the temporal reduction of the amplitude of the trailing pedestal has a similar effect on the measurements than the previously discussed depletion of the trailing pedestal by the amplified probe wave: it introduces a depletion of the actual probe gain measurement after the measurement is normalized using the probe gain without pulse in the fiber as reference, because the latter overestimates the contribution of the pedestal to the total gain experienced by the probe. Therefore, in much the same way as before, a specific depletion factor linked to this effect can be defined and used to calculate the BFS error induced in the measurements. Notice that the measurement distortion for EDFA II is larger than for EDFA I. This is due to the fact that the energy lost by the trailing pedestal due to its power reduction by the transient response of the EDFA is larger in EDFA II than in EDFA I because the recovery time of the gain is larger, as it can be seen in Fig. 12.

In order to estimate how these distortions affect on the sensor performance, the BFS along the fiber was measured for several ERs of the pump pulses in the system using EDFA I. Figure 14(a) and 14(b) show the resultant BFS distribution at the two hotspots along the link. Again, the probe power was kept low at -18.5 dBm in order to suppress the influence of pump and pedestal depletion on the measurements. Notice that a very significant BFS error is introduced by this effect, not only at the end of the FUT but even at the 5th kilometer, where the induced error is of a similar order to that at the end of the fiber. This response is caused by the distorted shape of the trailing pedestal due to the transient behavior of the EDFA explained in Fig. 12. Notice that the measurement in Fig. 14(b) displays some BFS variations before the hotspot start (indicated with a vertical dashed line) which was due to unintended strain introduced between measurements.



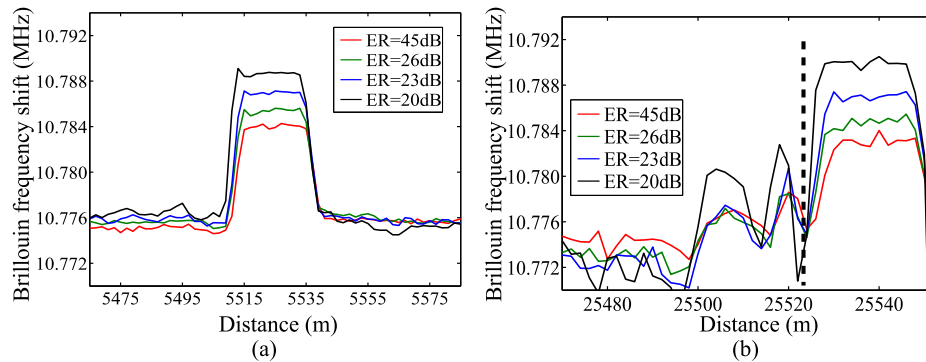


Fig. 14. Resultant Brillouin frequency shift along the hotspots deployed using the EDFA I: (a) hotspot I (b) hotspot II.

## 7. Conclusion

In conclusion, we have presented two non-local effects in BOTDA sensors, due to the pump pedestal depletion and the EDFA transient-induced pedestal distortion, that to the best of our knowledge had not been previously described. The non-local effect originated in the extra depletion of the trailing pulse pedestal have a magnitude that is of the same order than that coming from pulse depletion, and it introduces an impairment of identical nature to the measurement accuracy of the BOTDA sensor. For instance, it is found that, in a typical dual-probe BOTDA setup with 1-m spatial resolution, an  $ER > 32$  dB is needed to have less than 1-MHz BFS measurement error. Furthermore, the non-local effects due to the EDFA transient can be even more important depending on the particular EDFA device used. In addition, the limitation that they impose is independent of the probe wave power deployed; hence, they set an upper bound to the BOTDA sensor performance. Theoretical model calculations explain well the observed effects in both cases and match the experimental results.

In summary, these new effects have been shown to seriously impact BOTDA sensors that deploy EOMs to shape the pulses. Further research will be focused on investigating the significance of these effects in BOTDA systems deploying pump pulse coding. It is expected that the degradations imposed by the pedestal depletion will have a more pronounced impact in such systems because of the use of large sequences of pulses. This may impose even stringer constraints on the ER of the pulses deployed.

## Funding

Spanish Ministerio de Economía y Competitividad (TEC2013-47264-C2-2-R and TEC2016-76021-C2-1-R); FEDER funds; Universidad Pública de Navarra; German Research Foundation (DFG SCHN 716/13-1).